Korean J. Chem. Eng., 36(12), 2047-2059 (2019)
DOI: 10.1007/s11814-019-0392-x

pISSN: 0256-1115
eISSN: 1975-7220

A modified non-equilibrium lattice fluid model based on corrected fractional free volume of polymers for gas solubility prediction

Abolfazl Jomekian*,†, Bahamin Bazooyar, Seyed Jalil Poormohammadian***, and Parviz Darvishi*****

*Esfarayen University of Technology, North Khorasan, Esfarayen, Iran
**Department of Design and Engineering, School of Creative Arts and Engineering, Staffordshire University, Stoke-on-Trent, ST4 2DE, United Kingdom
***Chemical Engineering Department, School of Engineering, Yasouj University, Yasouj, Iran
(*Received 7 May 2019 • accepted 22 September 2019*)

Abstract−We propose a model based on non-equilibrium lattice fluid (NELF) theory and corrected fractional free volume of polymers to effectively and accurately predict the solubility of gases in different polymers. The method to achieve this purpose is based on the utilization of NELF model infinite dilution solubility coefficient (S_0) as the base of predictive calculations. To account for the isolated pore in the polymer matrix in density estimation, a fractional free volume correction factor (β) was introduced in NELF model. The modified NELF model was successfully applied for prediction of solubility of C_3H_8 and CO_2 in polyethylene oxide (PEO) and CO_2 in polyethylene terephthalate (PET), isotactic polypropylene (i-PP), polyetherimide (PEI), polymethyl methacrylate (PMMA) and polyethyl methacrylate (PEMA) with adjustments in β value and depth of diffusion of gases in polymer matrix (ζ) at different pressures and temperatures. This work involves multi-objective optimization using genetic algorithm of MATLAB toolbox with adjusted settings. It applies to find the optimum temperature at which the minimum standard deviation of β for different gas-polymer systems is obtained. β showed the same trend of change with temperature as the constrained pressure imposed on the amorphous phase in semi-crystalline polymers. A cubic correlation for standard deviation for β versus temperature was obtained which was able to anticipate the changing trend of β at different temperatures. The chi-square test results verified that compared with original NELF model, a more accurate model for prediction of gas solubilities in polymers has been proposed.

Keywords: NELF Model, Solubility Prediction, Infinite Dilution Solubility, Fractional Free Volume Correction Factor, Chi-square Test

INTRODUCTION

Most membrane gas separation industrial applications are conducted with the aid of polymeric membranes, which are flexible, accessible, and cheap with acceptable gas separation performance [1]. The transport of gases in polymeric membranes mainly follows a well-established solution-diffusion mechanism which defines the permeability of gas in membrane based on its solubility and diffusivity [2,3]. Therefore, information about the diffusivity and solubility of gases in polymers is of great importance for membranologists. The modeling of diffusion of gases in dense polymers is rather straightforward and mostly follows Fick's first law, conversely for prediction of solubility of gases in polymers; several different approaches have been applied by researchers such as investigation of volume of fluid [2,3], entropy generation analysis [4], Information Gap Decision Theory [5], field synergy analysis [6-8], utilization of committee machine intelligent system [9], modified van't Hoff-Arrhenius model [10], molecular dynamics simulation and free volume theory [11], modified Flory-Huggins model [12] and model based on non-equilibrium thermodynamics of glassy polymers [13]. Among these models, the thermodynamic models based on lattice fluid theory have attracted attention in recent years, especially for the prediction of solubility of gases in glassy polymers [14,15]. Due to the non-equilibrium nature of glassy polymers, non-equilibrium thermodynamics based models have been proposed for solubility prediction of gases in these polymers. Models such as the non-equilibrium models such as non-equilibrium lattice fluid (NELF) model [16], and the non-equilibrium statistical-associating-fluid theory (NE-SAFT) [17]. The NELF model, which is based on lattice fluid theory originating from the Sanchez and Lacombe equation of state, can also be applied to rubbery polymers [18]. The prediction ability of NELF model was improved by Doghieri and Sarti [19] for the nonequilibrium state of the glassy polymers. In their modified model the density of polymer was considered as an order parameter to evaluate the departure from equilibrium, and the solubility of gas in the polymer was calculated from the equivalency of chemical potentials of gas phase with dissolved gas in polymer matrix in a presumed pseudo-equilibrium condition. The fact that only initial polymer density was the criterion for distance from equilibrium was the main advantage of NELF, which makes it a powerful tool for precise prediction of solubility of gases in polymers. Hence, the research work on the modification of this model thrived in the last decade. De Angelis et al. [20] derived an expression for infinite dilution solubility based on the NELF model, for prediction of solubility

†To whom correspondence should be addressed.
E-mail: a_jomekian@esfarayen.ac.ir

of different gases in polysulfone, polycarbonate, polymethyl methacrylate, etc. Minelli and De Angelis [21] proposed a Sanchez-Lacombe equation of state base model for gas solubility prediction in polymers with a constraint pressure parameter for describing the effect of crystal portions in considered semi-crystalline polymers. The combination of NELF model with the Sanchez Lacombe equation of state was used by Minelli [22] as a new approach to predict the solubility of CO_2 in polyethylene terephthalate (PET). Galizia et al. [23] predicted the solubility of H_2 and He in glassy and rubbery polymer based on LF and NELF models utilizing infinite dilution solubility coefficient with only one adjustment parameter, and good agreement between experimental data and the applied model has been observed at the range of pressure and temperature investigated in their work. Minelli and Doghieri [24] proposed a predictive model based on the improvement of NELF model by a model proposed for sorption induced volume dilation in glassy polymers. This modified version of NELF model was able to predict the solubility of different gases in glassy polymers at high pressure with non-ignorable volume dilation of the polymer. In many gas-polymer systems considered for determination of NELF model parameter, the sorption of CO_2 was one the mostly investigated subjects. It was due to the fact that the exigency of the capture of CO_2 and accordingly the knowledge about the sorption behavior of this gas in different polymers is thoroughly perceived, since CO_2 is the origin of many industrial problems such as heat value reduction, hydrate formation, pipeline corrosion and environmental issues such as global warming and ocean acidification [25,26].

The optimization of the thermodynamic models with evolutionary algorithms to find the optimum parameters and conditions of the model was applied by researchers in recent years [27,28]. Genetic algorithm (GA) is one of these evolutionary algorithms used in optimization in computer programs such as MATLAB. Using this method has several advantages over conventional optimization methods and algorithms. This method offers practical benefits to the researcher facing difficult optimization problems. These benefits are multifaceted, including the simplicity of the approach, its robust response to different circumstance and its flexibility. GA also offers a set of procedures that may be usefully applied to problems that have diverged by common traditional techniques. For instance, in the current work with the modified NELF models, due to the diversity of gas-polymer solubility data which makes it difficult for the conventional optimization algorithm to converge to an acceptable solution, utilization of GA seems an effective approach in finding an optimized solution.

In most of the works on modification of the NELF model, one or two adjustable parameters are defined to aid the model to fit the experimental data based on the thermodynamic properties of considered gas-polymer systems [29]. In this work, as the first novel approach, the fractional free volume (f) of the polymers, which is a very important factor in determination of infinite dilution solubility coefficient, is proposed. A correction factor (β) for consideration of isolated pores in the measurement of free volume of polymers was introduced in the calculation of solubility coefficient (S) from infinite dilution solubility coefficient (S_0). Different gas-polymer systems were selected for prediction of solubility of gases in different polymers.

As the second novel approach, for optimization of the results obtained in modeling part of this study, the genetic algorithm multi-objective optimization with customized setting was applied to find the optimum condition for prediction of solubility of gases in different polymers followed by derivation of a relationship for anticipation of fractional free volume correction factor with temperature from the result of accomplished multi-objective optimization.

THEORETICAL BACKGROUND

The NELF model can be applied to polymers at temperatures above their T_g or in fact to amorphous equilibrium phases as well as at room temperature in which the glassy polymers are at non-equilibrium state. The characteristic parameters of LF theory (P*, T*, ρ*) and the mixing rules for defining the behavior of the pure components are also valid for NELF model. Considering that the sorption of CO_2 and C_3H_8 generally causes plasticization or swelling in polymers with high affinity for these gases, the polymer density varies significantly with increase in sorption of these gases, mainly due to the increased flexibility of polymeric chains which leads to the increase in free volume of the polymer. Therefore, the polymer density only can be estimated accurately at low pressures where the infinite dilution can be assumed. At these low pressures the NELF model shows remarkable predictive behavior as stated by De Angelis et al. [20]; therefore, a relationship for infinite dilution solubility coefficient (S_0) can be derived based on Helmholtz free energy of the non-equilibrium glassy phase.

The dimensionless Helmholtz free energy of gas mixture based on lattice fluid theory can be expressed by the following equation [21,30,31]:

$$\frac{A}{rNRT^*} = -\tilde{\rho} + \tilde{T}\left[\left(\frac{1}{\tilde{\rho}} - 1\right)\ln(1-\tilde{\rho}) + \frac{1}{r}\ln(\tilde{\rho}) + \sum_i \frac{\phi_i}{r_i}\ln(\phi_i)\right] \tag{1}$$

Eq. (2) can be used to calculate the chemical potential per unit mass of gas molecule i dissolved in polymeric phase by the following relationship [30]:

$$\mu_i^{NE} = \left(\frac{\partial a^{NE}}{\partial \rho_i}\right)_{T,\ \rho_{j\neq i},\ \rho_{pol}} \tag{2}$$

Therefore, the resulting non-equilibrium chemical potential μ_i^{NE} can be calculated as follows [21,30,31]:

$$\begin{aligned}\frac{\mu_i^{NE}}{RT} &= \ln(\tilde{\rho}\phi_i) - \ln(1-\tilde{\rho})\left[r_i^0 + \frac{r_i - r_i^0}{\tilde{\rho}}\right] \\ &\quad - r_i - \tilde{\rho}\frac{r_i^0 v_i^*}{RT}\left[p_i^* + \sum_{j=1}^{N_c+1}\phi_j(p_j^* - \Delta p_{i,j}^*)\right]\end{aligned} \tag{3}$$

Under low pressures where gas is hardly dissolved in a glassy polymer, Eq. (4) is applied for determining the infinite dilution solubility coefficient [32]:

$$S_0 = \lim_{P\to 0}\frac{C_1}{P} \tag{4}$$

where C_1 is a measure of solute concentration in the polymeric mixture. In this state, the gas-polymer density reduces to the density of polymer. Therefore, since swelling does not occur at infinite

dilution pressure, the solubility coefficient can be expressed as follows for glassy polymers under non-equilibrium conditions [20,32]:

$$\mathrm{Ln}(S_0)=\mathrm{Ln}\left(\frac{T_{STP}}{p_{STP}T}\right)+r_1^0\left\{\left[1+\left(\frac{v_1^*}{v_2^*}-1\right)\frac{\rho_2^*}{\rho_2^0}\right]\mathrm{Ln}\left(1-\frac{\rho_2^0}{\rho_2^*}\right)+\left(\frac{v_1^*}{v_2^*}-1\right)+\frac{\rho_2^0 T_1^*}{\rho_2^* T}\frac{2}{p_1^*}\Psi\sqrt{p_1^* p_2^*}\right\} \tag{5}$$

where subscript 1 is related to the properties of gaseous penetrant and subscript 2 is representative of polymer properties. v_i^*, ρ_i^*, p_i^* and T_i^* are characteristic parameters of either gas or polymer, which are volume, density, pressure, and temperature in respective order. T_{STP} and P_{STP} are the standard temperature and pressure, respectively, and Ψ is the binary interaction parameter. In the absence of reliable data for this parameter, it is reasonable to assume Ψ=1 [28]. ρ_2^0 is the density of polymer under very low pressures. This parameter is nearly the same as the pure polymer density because at low pressures the gas sorption in the polymer is not significant. Therefore, the swelling or plasticization phenomena do not affect the density of the polymer. The value of pure polymer density for various polymers can be found in the literature [16-18]. In infinite dilution state, the volume fraction of polymer (φ_2) approaches unity and the volume fraction of dissolved gas approaches a negligible value which is equal to the molecular diffusion of gas in polymer [33]. Hence the solubility coefficient can be written as:

$$S=S_0\frac{\varphi_1}{j_1\varphi_2} \tag{6}$$

Assuming that the ideal gas law is valid for infinite dilution state, which is a reasonable assumption considering the very low pressure applied, the molecular diffusion of gas into the polymer can be expressed by the Fick first law of diffusion:

$$j_1=-D_{12}\frac{dC_1}{dz}=-\frac{D_{12}}{RT}\frac{dP}{dz}=-\frac{D_{12}\Delta P}{RT\,\zeta} \tag{7}$$

where C_1 is the concentration of gas in polymer, z is the direction of diffusion and D_{12} is the diffusivity of gas in polymer which is calculated based on the following formula [34]:

$$D_{12}=\frac{10^{-4}\left(1.04-0.249\sqrt{\frac{1}{M_1}+\frac{1}{M_2}}\right)\left(\sqrt{\frac{1}{M_1}+\frac{1}{M_2}}\right)T^{1.5}}{P(r_{12})^2 f\left(\frac{kT}{\varepsilon_{12}}\right)} \tag{8}$$

where T is temperature (K), r_{12} is the molecular separation at collision in (nm), M is the molecular weight (kg mol^{-1}), k is Boltzmann's constant, f is collision function and ε_{12} shows the energy of molecular attraction (kg m^{-2} s^{-2}).

The φ_1 is defined by the characteristic parameter of gas and fractional free volume by the following equation:

$$\varphi_1=\frac{-\rho^*\rho_2^*+f\rho^*\rho_2^*+\rho_2^*\rho_2^0}{-\rho^*\rho_2^*+f\rho^*\rho_2^*+\rho_2^*\rho_2^0-\rho_1^*\rho_2^0} \tag{9}$$

And φ_2 is defined by the characteristic parameter of polymer and fractional free volume by the following equation:

$$\varphi_2=\frac{-\rho_1^*\rho_2^0}{-\rho^*\rho_2^*+f\rho^*\rho_2^*+\rho_2^*\rho_2^0-\rho_1^*\rho_2^0} \tag{10}$$

The following relationship based on fractional free volume was applied for definition of ρ^*:

$$\frac{1}{\rho^*}=\frac{(1-f)\rho_2^*}{\rho_1^*\rho_2^*(1-f)+\rho_2^*\rho_2^0-\rho_1^*\rho_2^0} \tag{11}$$

MODELING AND OPTIMIZATION

To account for the isolated and inaccessible pores in the polymer structure, a correction factor (β) for estimation of fractional free volume as the first adjustable parameter was defined as follows:

$$\beta=\frac{f}{\left(\frac{\rho^*-\rho_2}{\rho^*}\right)} \tag{12}$$

The depth of diffusion in infinite dilution solubility was considered the depth in the matrix of polymer in which the applied pressure approaches zero; this parameter (ζ), as it was previously introduced, was regarded as the second adjustable parameter.

A multi-objective optimization by the genetic algorithm was uti-

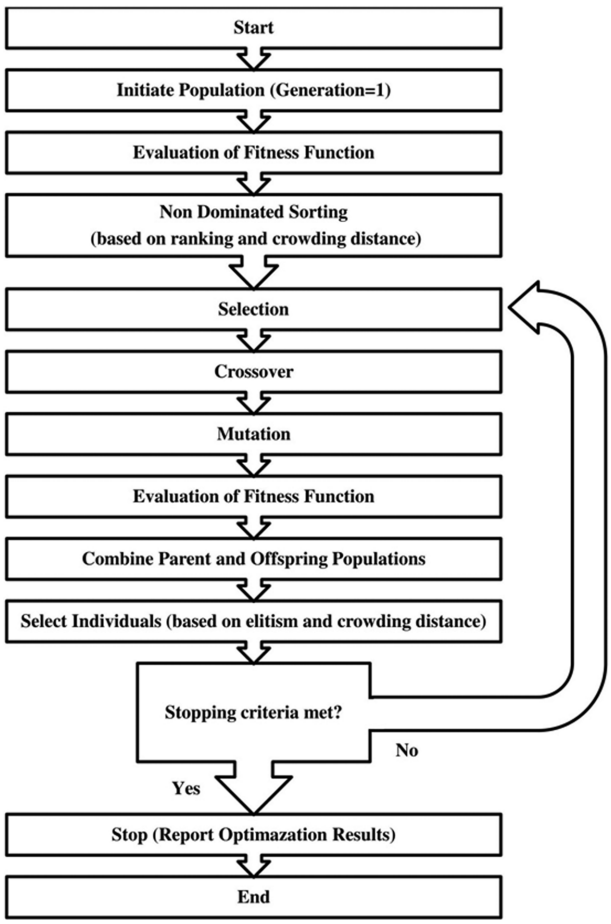

Fig. 1. The cascade flowchart of applied genetic algorithm multi-objective optimization.

lized to determine the optimum temperature at which there is an excellent agreement between experimental and modeling data.

The genetic algorithm multi-objective function optimizers try to minimize the difference between model and experimental data considering the following constraints:

$$0 \le \beta \le 1$$
$$\zeta \ge 0 \qquad (13)$$
$$273 \le T \le 573$$

The flowchart representing the algorithm that was followed in this study in optimization based on elitist non-dominated sorting genetic algorithm (NSGA-II) is presented in Fig. 1. This most widely used algorithm, which applies the elitism concept in the non-dominated sorting algorithm, is able to solve constrained and non-constrained multi-objective optimization problems due to its enhanced convergence properties. In the first step of the algorithm the initial population is generated, then the most important part of optimization, which is the definition of the fitness function for minimization, is performed. The fitness function was defined based on the relationship obtained for β values with temperature for each gas-polymer case at different temperatures investigated. The fitness function was defined as a matrix with different columns in which each column was assigned to each temperature-dependent β value obtained from different solubility isotherms for each gas-polymer system considered. Afterwards, the individual selection in the population was performed based on ranking and crowding distance. The NSGA-II algorithm uses crossover and mutation genetic operators in order to create a new population. The next step is the combination of a newly generated population with the older one then individual selection is performed based on elitism and crowding distance. Finally, if the results satisfy the stopping conditions, the loop ends and the result of optimization are produced, otherwise the loop goes back to the selection step and next population is generated. The single stopping criterion for the case of this study was if the maximum number of generations (100) is exceeded.

While there are many good genetic algorithm packages such as Python, none of them provides a domain that is compatible with the existing tools of optimization. MATLAB, on the other hand, has the advantage of being compatible with different control and optimization software. Hence, MATLAB global optimization toolbox was used for multi-objective optimization using a genetic algorithm. The settings for optimization using 'gamultiobj' solver are presented in Table 1.

Table 1. The genetic algorithm multi-objective optimization preferences in global optimization toolbox of MATLAB software

Variables	Values
Population size	15
Creation function	Constraint dependent
Initial population	20
Selection function	Tournament
Tournament size	10
Crossover fraction	0.9
Mutation function	Constraint dependent
Crossover function	Intermediate
Crossover ratio	1
Pareto front population fraction	0.4
Number of generations	100

Table 2. The characteristic parameters of NELF model for the gases and polymers considered

Gas/Polymer	T^* (K)	p^* (MPa)	ρ^* (g/cm^3)	Reference
C_3H_8	375	320	0.690	[21]
CO_2	300	630	1.515	[21]
PEO	590	620	1.209	[21]
PET	735	780	1.425	[22]
PMMA	695	560	1.270	[33]
PEMA	602	567	1.221	[35]
PEI	820	610	1.384	[24]
i-PP	692	298	0.883	[21]

Table 3. The calculated infinite solubility coefficients for investigated gas-polymer systems

Polymer / Gas	PEO	PET	PMMA	PEMA	PEI	i-PP
CO_2	7.98	6.67	3.85	3.96	7.72	3.75
C_3H_8	269.3	224.90	142.12	159.32	217.62	150.28

RESULTS AND DISCUSSION

1. Modeling

The lattice fluid characteristic parameters of considered gases (T_1^*, p_1^* and ρ_1^*) and the investigated polymers (T_2^*, p_2^* and ρ_2^*) were extracted from different sources and presented in Table 2. The calculated infinite solubilities at 30 °C by Eq. (5) for each pair of the polymer-gas system are presented in Table 3.

The values of infinite dilution solubilities calculated for propane are higher than that of carbon dioxide. The phase of heavier hydrocarbons tends to change from the gas phase to liquid, and the solubility of liquid in polymers is significantly higher than the solubility of gases. This is because propane has a tendency to convert from vapor to liquid phase during sorption in polymers. Since the solubility of the condensed phase is higher in polymers compared with vapors, the infinite dilution solubility of C_3H_8 shows significantly higher values compared with that of CO_2.

1-1. Solubility of Gases in PEO

The solubility isotherms of C_3H_8 in molten PEO can be observed at three different temperatures in Fig. 2(a).

PEO is a versatile polymer that has shown potential in many applications from gas separation membrane to PEM fuel cells and from cosmetics to petrochemicals. The low melting point of this semi-crystalline polymer provides the possibility of utilization of its full amorphous properties at relatively low temperatures (T>50 °C). The polyether group in PEO shows high affinity for light hydrocarbon sorption, hence numerous reports regarding application of this polymer as hydrocarbon separation membrane can be found in literature in recent years. The experimental data for solubility of

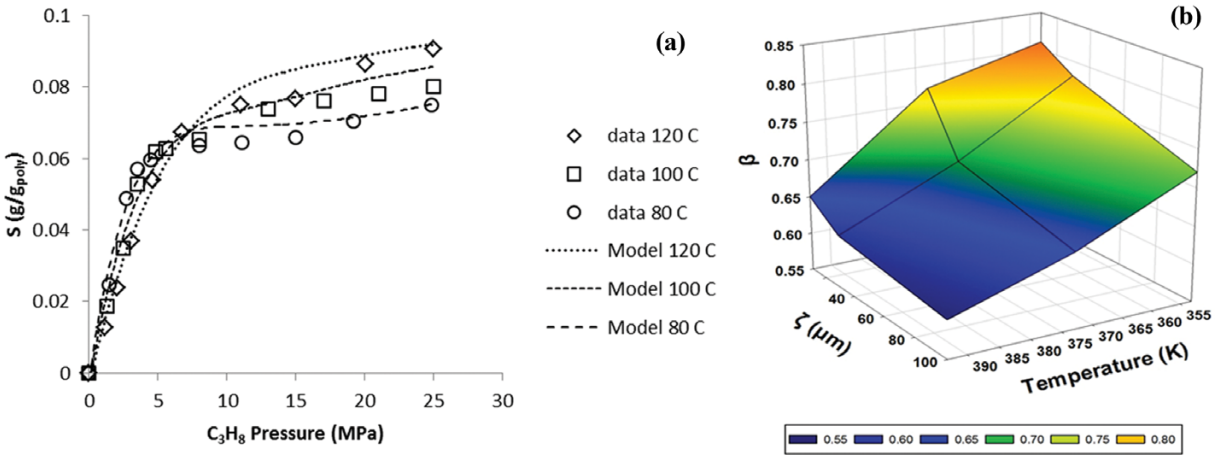

Fig. 2. (a) The predictions of solubility isotherms for C_3H_8 in PEO: experimental data by Wiesmet et al. [36] (b) The calculated values for adjustable parameters β with ζ and temperature.

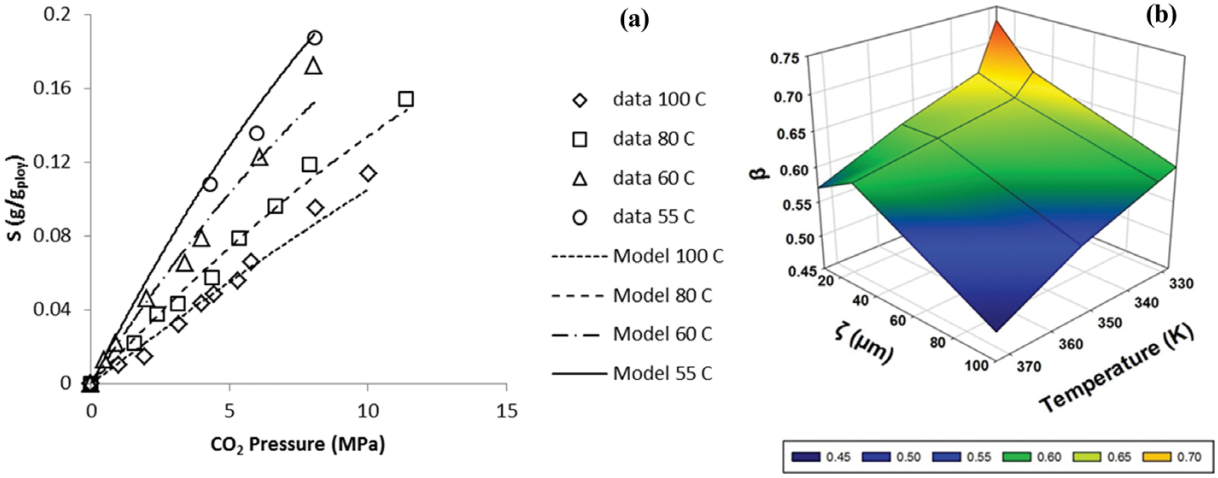

Fig. 3. (a) The predictions of solubility isotherms for CO_2 in PEO: experimental data by Wiesmet et al. [36] (b) The calculated values for adjustable parameters β with ζ and temperature.

C_3H_8 in PEO were extracted from Wiesmet et al. [36]. Their experimental work was focused on low molecular weight PEOs (PEG4000 and PEG8000). It is observed that at low concentration of solute in PEO, the effect of chain length of PEO in sorption of gas vanishes. Therefore, the solubility under 10 wt% of C_3H_8 is not dependent on the type of PEO examined.

As can be observed, there is very good agreement between model and experimental data. This is because of the corrected (reduced) FFV of semi-crystalline polymers which were considered in modeling of sorption behavior of gases. The effect of correction factor of fractional free volume is similar to the effect of hypothetical constraint pressure that was taken into the account in some previous studies on the solubility of gases in these polymer [21]. The hypothetical constraint pressure imposed on amorphous phase from a crystalline portion of the polymer causes the reduction of FFV of semicrystalline polymers; hence the introduction of the corrected coefficient of FFV (β) prevents the model from the overestimation of solubility of C_3H_8 in PEO. The dependency of β on the depth of diffusion and temperature is presented in Fig. 2(b). As can be seen, the value of β decreases with increase in depth of diffusion and rise in temperature; this is because as the depth of diffusion increases, the diffusion of gas molecule in the matrix of polymer faces more difficulties due to the increased interaction with polymer chains [37]; thus its effect is similar to the reduction of FFV of polymer. On the other hand, with an increase in temperature, as can be seen in Fig. 2(a), at most of the investigated pressures the sorption capacity of PEO increases, which means the reduction of hypothetical imposed constraint pressure on the PEO matrix [21] and thereafter increases in FFV of a polymer leading to a reduction in correction factor β with temperature.

For the case of CO_2 sorption in molten PEO, as can be seen in Fig. 3(a) and (b), the model was properly fitted to the experimental data and compared with C_3H_8 sorption in the PEO case. Almost the same trend of change of β with ζ and T can be observed for CO_2 sorption. This is most probably because the depth of diffusion in PEO has almost the same effect on both of these gases, considering the similar molar mass of these gases. As it is clear according to Graham's law of diffusion, as the molecular weight of a penetrat-

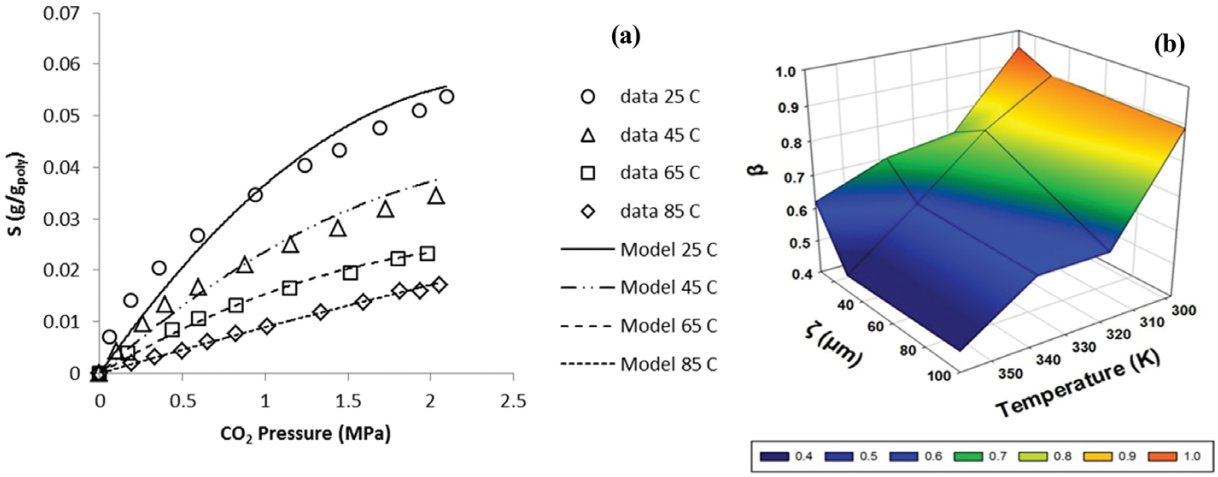

Fig. 4. (a) The predictions of solubility isotherms for CO_2 in PET at low temperatures: experimental data by Koros et al. [39-42] (b) The calculated values for adjustable parameters β with ζ and temperature.

ing gas increases its diffusion rate decreases in diffusion medium and vice versa. Therefore, it is expected that the molecules with the same molecular weight have been affected similarly by diffusion medium structure. On the other hand, a similar effect of temperature on β in both CO_2 and C_3H_8 sorption cases can be explained by the Stokes-Einstein equation and Thran et al. [38] correlation of fractional free volume in terms of diffusivity of gas in polymer. According to the Stokes-Einstein equation, the diffusivity in polymer is proportional to the temperature at which the diffusion occurs and based on Thran et al. correlation, the inverse of the fractional free volume is exponentially related to the diffusivity of gas in polymer. Therefore the diffusivity of gas in polymer is affected by temperature and the fractional free volume is affected by diffusivity of gas in polymer. Because the diffusion of CO_2 and C_3H_8 in PEO is almost similar due to the as-explained reasons, the effect of temperature on fractional free volume of PEO is almost similar in both sorption cases investigated.

1-2. Solubility of CO_2 in PET

Fig. 4(a) presents the solubility isotherms of CO_2 along with the predicted solubility curves in PET at low temperatures.

The CO_2 solubility isotherms below T_g show downward curvatures for all of the investigated temperatures, due to excess of the free volume of the polymer in the glassy state [22]. As can be seen in these isotherms with increase in temperature, the curvature of the isotherms is reduced with pressure and the isotherms become more linear. This is because of the reduced distance from glass transition temperature, which leads to the occurrence of the second-order glass-rubber transition at lower CO_2 pressures, this results in nearly linear isotherms at lower pressures for isotherms at higher temperatures [39-41]. This partially affects the predictive performance of the modified NELF model. As can be seen the effect of second-order glass-rubber transition at lower temperatures (25 °C and 45 °C) on density or in fact the free volume of PET at intermediate applied pressure (≈1 MPa) leads to the transition of the predictive performance of the model from underestimating to overestimating. In fact, the experimental data were subjected to abrupt change in fractional free volume at second-order glass-rubber transition temperature, which was not considered in the model; however, at higher pressure the model approaches the experimental data because the effect of second-order glass-rubber transition vanishes. In Fig. 4(b), the β value decreases with increase in temperature; the reason is related to the fact that the increase in temperature because of the exothermic nature of the sorption of CO_2 in PET, the rise in temperature leads to a reduction in sorption capacity of PET. In the modified NELF model, this behavior is described by means of a decrease in density and an increase in FFV of the polymer. The increase in FFV results in rising in the diffusion of gas molecules; this rise in diffusion causes the solubility to overestimate experimental data based on Eq. (6) if the correction factor of FFV was not involved. Hence, it was observed that β decreases with rising temperature.

The CO_2 solubility in PET at temperatures above T_g (95, 105 and 115 °C) is shown in Fig. 5(a), which presents the typical behavior for gases in rubbery polymers, well described by Henry's law. Therefore, nearly linear predicted sorption isotherms are observed in this figure.

The slopes of these linear isotherms are slightly different from each other; this means that minor changes in density and FFV of membranes occurred within the temperature range considered. Hence, as can be seen in Fig. 5(b), a linear drop in β values with temperature is also observed. A rise in β can be observed with the depth of diffusion in PET, which is an opposite trend of change when compared with PEO and other cases. The reason can be related to the low affinity of PET for CO_2 sorption. As the depth of diffusion increase the CO_2 sorption becomes more difficult in PET; however, when CO_2 sorption reached a certain value in the depth it penetrated, the amorphous PET matrix started to crystallize and at the same time the mobility of PET chains increased due to the partial plasticization occurrence as a side effect of dissolved CO_2. It is well-known that the crystal portion of polymer is unwilling to dissolve CO_2 [43]; hence the formed crystals excluded CO_2 out of PET matrix, which leads to lower dissolved CO_2 concentration. This phenomenon cannot be observed in other CO_2 sorption systems investigated, and this can be the reason for unique trend

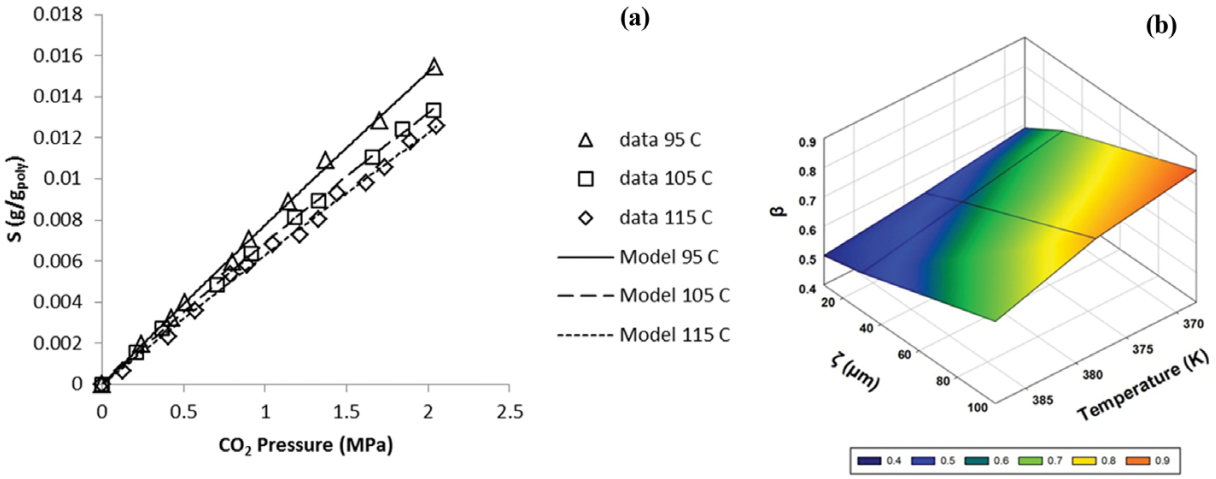

Fig. 5. (a) The predictions of solubility isotherms for CO_2 in PET at high temperatures: experimental data by Koros et al. [39-42] (b) The calculated values for adjustable parameters β with ζ and temperature.

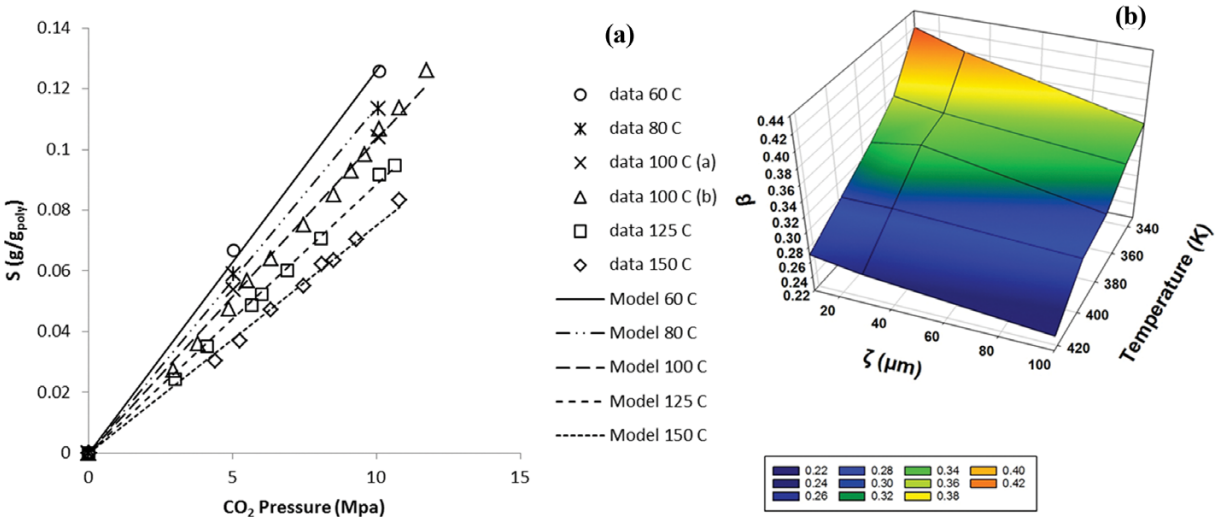

Fig. 6. (a) The predictions of solubility isotherms for CO_2 in i-PP at low temperatures: experimental data by Li et al. [44] and Lei et al. [45] (b) The calculated values for adjustable parameters β with ζ and temperature.

of change of β with depth of diffusion in the matrix of PET.

1-3. Solubility of CO_2 in i-PP

Isotactic polypropylene (i-PP) is one of the polyolefins of great interest in many practical applications. Fig. 6(a) shows the isotherms of CO_2 sorption in i-PP at different temperatures below melting point of this polymer extracted from works by Li et al. [44] and Lei et al. [45]. As can be seen, the modified NELF model was able to successfully predict the solubility of CO_2 in i-PP. This is because the crystallinity degree of this polymer is high at investigated temperatures; hence the hypothetical constrained pressure imposed on amorphous parts of polymer structure must be high for model to comply with experimental data [21], and there is a decreasing trend of change of constrained pressure with temperature due to the reduction of crystallinity degree of polymer and increase in its amorphous phase. This means that the FFV of polymer increases with temperature; hence similar to the CO_2 sorption in PEO, the correction factor of FFV must decrease with temperature to prevent the model from overestimating the experimental data point, as can be seen in Fig. 6(b). Another noteworthy point in Fig. 6(b) is that the values of β are relatively far from unity even at its maximum; the reason for this result is that the sorption data of CO_2 in i-PP are reported at very high pressures. This high applied pressure has significant effect on density and FFV of polymer examined leading to the overestimation of FFVs by NELF model in higher pressures as it was observed by Minelli et al. [31] for solubility of CO_2 in PEO case; hence, smaller correction factors of FFV must be applied to the model.

The experimental solubility isotherms of CO_2 in molten i-PP along with the predicted solubilities with modified NELF model can be observed in Fig. 7(a).

As can be seen, the model was able to accurately describe the CO_2 sorption isotherms which were extracted from two separate works by Li et al. [46] and Chen et al. [47] in molten i-PP. Even at high pressures, the model is properly fitted to experimental data

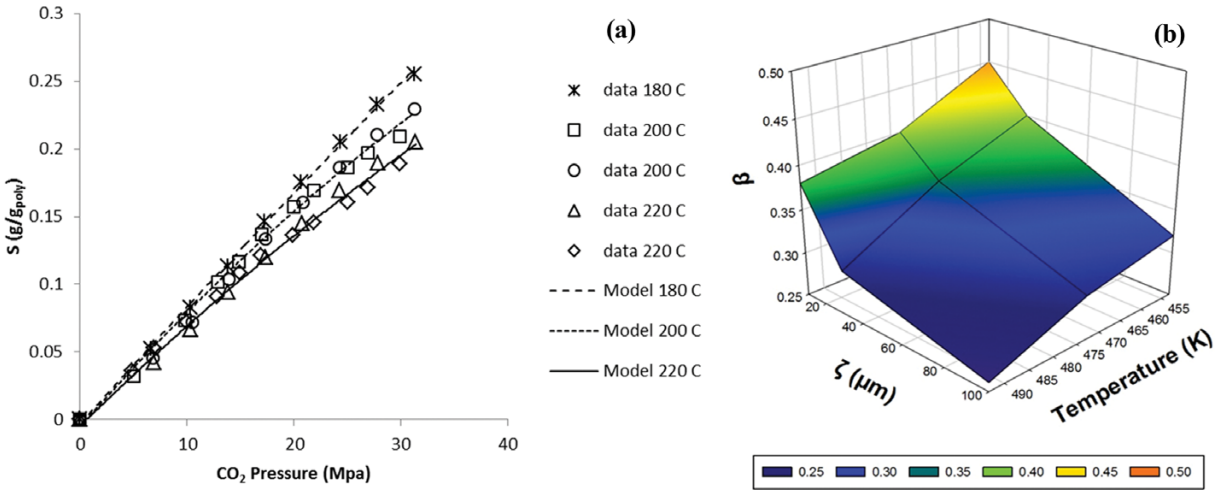

Fig. 7. (a) The predictions of solubility isotherms for CO_2 in i-PP at high temperatures: experimental data by Li et al. [46] and Chen et al. [47] (b) The calculated values for adjustable parameters β with ζ and temperature.

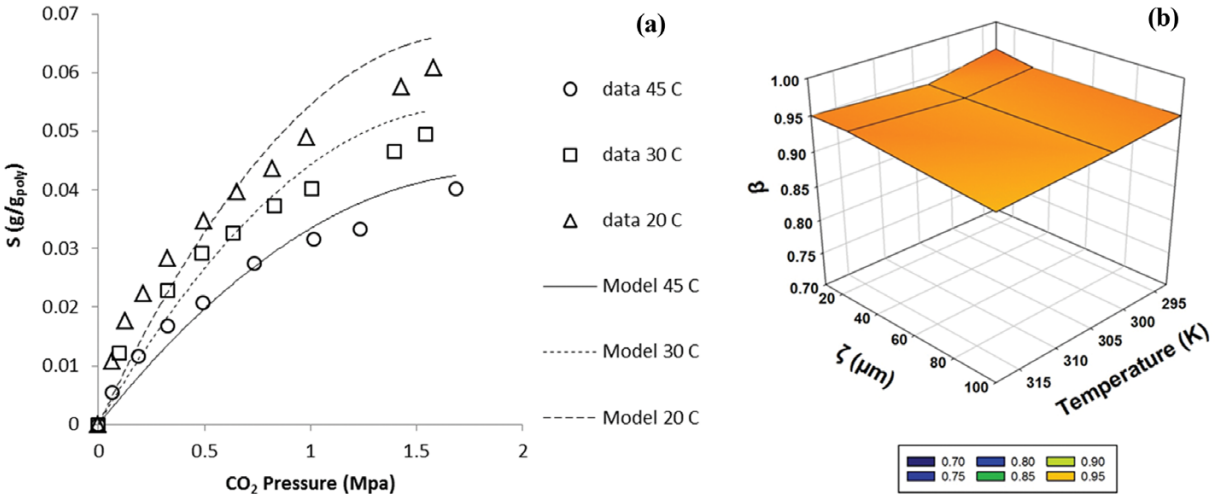

Fig. 8. (a) The predictions of solubility isotherms for CO_2 in PEI: experimental data by Lopez-Gonzalez et al. [48] (b) The calculated values for adjustable parameters β with ζ and temperature.

points that were not observed in Minelli and Di Angelis [21] at 180 °C who calculated a constant binary interaction parameter in different temperatures investigated. In this work, because of the high pressure applied in sorption experiments by Li et al. [46] and Chen et al. [47], it is believed that FFV is significantly affected by pressure; therefore, the depth of diffusion becomes shorter and accessing the matrix of bulk of i-PP is more difficult for CO_2 molecules. Hence as can be observed in Fig. 7(b), there can be seen very low values for β with increase in ζ values from 10 to 100 μm.

1-4. Solubility of CO_2 in PEI

Polyetherimide (PEI) is a renowned membrane of the polyimide family. This polymer, which has high glass transition temperature (≈217 °C), is widely used as membrane material for gas, especially CO_2 separation purposes. Fig. 8(a) presents different CO_2 solubility isotherms extracted from Lopez-Gonzalez et al. [48] at 20, 30 and 45 °C in the pressure range up to about 2 MPa in glassy PEI.

As can be observed in Fig. 8(a), the model does not show a very accurate estimation of CO_2 solubilities in PEI, and there are deviations at both high and low pressures from experimental data points. The reason can be related to the fact that for PEI Henry's law is not valid. The sorption of CO_2 in PET can be described more accurately by the dual-mode sorption model, demonstrating that CO_2 molecules do not only dissolve in the polymer matrix, but can also be present in the excess free volume of PEI [49]. Hence, there exists a hysteresis for the sorption of CO_2 in PEI. Desorption values are in higher then sorption values, especially at higher pressure due to the enhanced sorption of CO_2 in PEI. During desorption, the collapse of the free volume takes more time than the desorption of CO_2 [50]. Consequently, a higher amount of free volume is available during desorption, resulting in higher CO_2 concentrations. Therefore, it can be said that the model predicts the solubility of CO_2 in PEI more accurately at high pressures based on desorption data points if it was available.

Fig. 8(b) shows that there is almost a constant value for β at dif-

ferent ζ. According to Simons et al. [49] the thickness of PEI film does not have a significant effect on the CO_2 sorption capacity of PEI. This implicitly demonstrates that the depth of diffusion of CO_2 in the matrix of PET does not have a significant effect on the solubility of CO_2 in PEI.

1-5. Solubility of CO_2 in PMMA and PEMA

Polymethyl methacrylate (PMMA) and polyethyl methacrylate (PEMA) are methacrylate resins. Both of these polymers have been investigated for CO_2 sorption and separation in numerous research works due to their high affinity for CO_2. Fig. 9(a) demonstrates three different CO_2 solubility isotherms in PMMA extracted from Koros et al. [51] along with the prediction by modified NELF model in the pressure range up to about 2.5 MPa in PMMA. As can be seen, the model was able to successfully predict the solubility of CO_2 in PMMA similar to Minelli and Doghieri [24], who found that the binary interaction parameter between CO_2 and PMMA was constant and independent of temperature. In this work, although the correction factor of FFV is dependent on temperature as it can be observed in Fig. 9(b), the range of change of β is very limited (about 2%) at each diffusion depth considered. This result is in very good agreement with the results of Minelli and Doghieri [24], demonstrating an almost temperature-independent interaction between CO_2 and PMMA. This is related to the fact that some rheological properties of PMMA remain constant with the variation of temperature. As it is observed in several different studies, the steady-state recoverable compliance of PMMA, which shows the ability of PMMA to recover its original structure after bearing mechanical stress, is independent of temperature [52, 53]. Because the solubility of gas in polymer is affected by change in rheological properties of polymer, the temperature independency

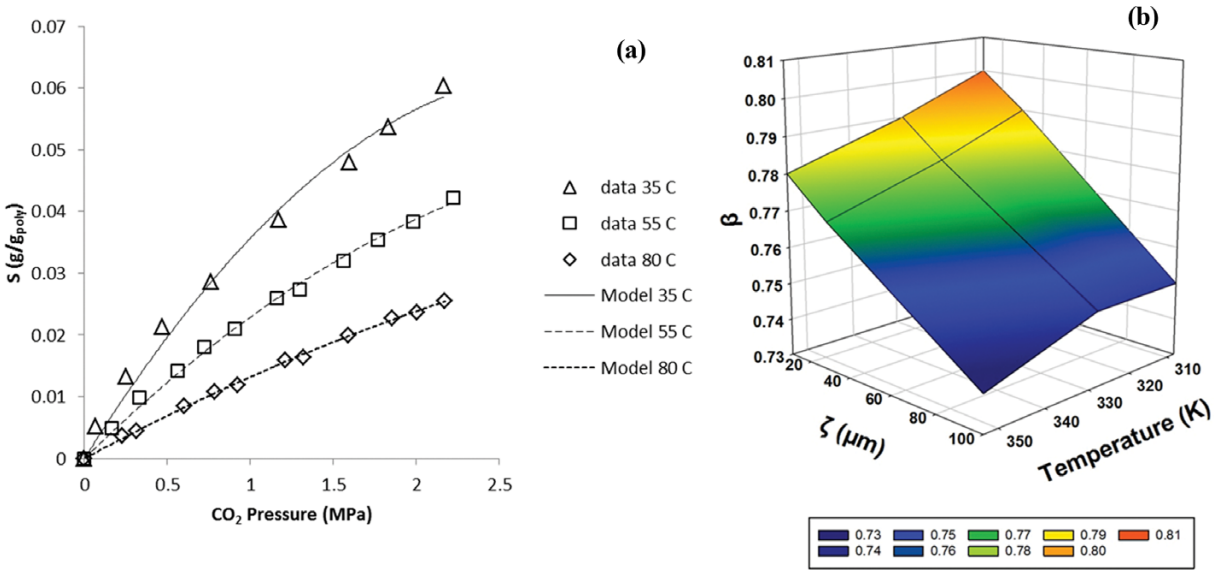

Fig. 9. (a) The predictions of solubility isotherms for CO_2 in PMMA: experimental data by Koros et al. [51] (b) The calculated values for adjustable parameters β with ζ and temperature.

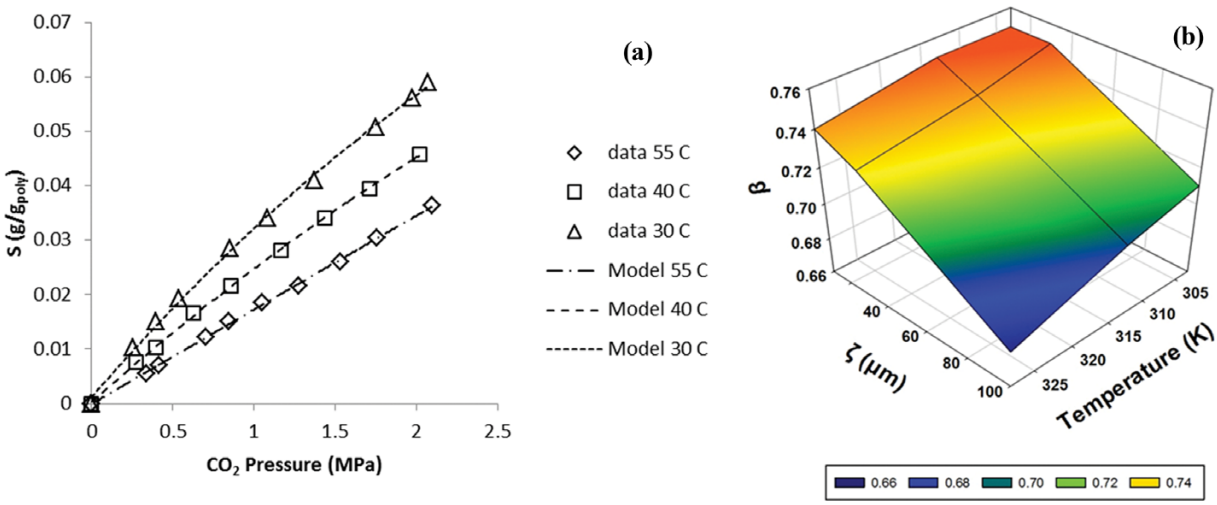

Fig. 10. (a) The predictions of solubility isotherms for CO_2 in PEMA: experimental data by Koros et al. [51] (b) The calculated values for adjustable parameters β with ζ and temperature.

Table 4. Summary of the constants of correlations for β parameter obtained from the results of modified NELF model for different gas-polymer systems

Polymer/Gas	β=a T^2+b T+c								
	ζ=10 μm			ζ=30 μm			ζ=100 μm		
	a	b	c	a	b	c	a	b	c
PEO/C_3H_8	-1×10^{-4}	0.0706	−11.651	2×10^{-5}	−0.0226	5.6602	3×10^{-5}	−0.0217	5.2472
PEO/CO_2	5×10^{-5}	−0.038	7.18169	3×10^{-5}	−0.0191	4.2056	-2×10^{-5}	0.0129	−1.2787
l-PET/CO_2	9×10^{-5}	−0.0625	11.793	0	−0.0076	3.1778	-6×10^{-5}	0.0333	−3.4671
h-PET/CO_2	-1×10^{-4}	0.1109	−19.948	-5×10^{-4}	0.366	−66.206	-2×10^{-4}	0.1805	−31.718
l-i-PP/CO_2	1×10^{-5}	−0.0103	2.563	1×10^{-6}	−0.0024	1.0552	-4×10^{-6}	0.0016	0.2224
h-i-PP/CO_2	4×10^{-5}	−0.0372	9.6176	-2×10^{-5}	0.0211	4.0507	-2×10^{-5}	0.0221	4.5837
PEI/CO_2	1×10^{-4}	−0.0656	11.016	7×10^{-5}	−0.0407	7.1616	1×10^{-5}	−0.0089	2.4267
PMMA/CO_2	0	−0.0004	0.9359	0	−0.0004	0.9259	-9×10^{-6}	0.0057	−0.148
PEMA/CO_2	-3×10^{-5}	0.0164	−1.779	1×10^{-5}	−0.0092	2.3175	0	−0.0012	1.0776

of steady-state recoverable compliance of PMMA leads to nearly temperature independency of solubility of CO_2 in PMMA.

Fig. 10(a) demonstrates three different CO_2 solubility isotherms in PEMA extracted from Koros et al. [51] along with the prediction by modified NELF model.

As can be seen, similar to the CO_2/PMMA system, the model was able to accurately predict the solubility of CO_2 in PEMA at temperatures below its T_g. Fig. 10(b) is also very similar to Fig. 9(b), which means the mechanism of sorption of CO_2 in PEMA and PMMA is almost the same. This is mainly because of the similar chemical structure and physical properties of these two methacrylate-based polymers. The sorption enthalpies of these two polymers are in a very close range (2-4 kcal mol^{-1}) based on Koros et al. [51], meaning that the solubility of CO_2 in these polymers is similar from a thermodynamics point of view.

2. Optimization

A summary of the correlations for β in terms of temperature at different values of ζ for different gas/polymer systems is presented in Table 4.

The quadratic form of the temperature-dependent equation was fitted to the calculated β values at different ζ and the constant of the equation is presented in Table 4. As can be seen, the value of constant 'a' for almost all of the considered systems is very small compared to values of 'b' and 'c'. This demonstrates that the regression curves are almost linear with a mild curvature. In fact, some of the 'a' values in the table approach zero. This suggests that the dependency of β at different depth of diffusion can be expressed by a simple quadratic or linear equation. Hence, values of β at excluded temperatures can be easily estimated with a high level of confidence.

A fitness function in MATLAB environment was defined including all of the equations presented in Table 4 with temperature as input and β values as output in 27 vectors. Then, genetic algorithm multi-objective optimization with global optimization toolbox of MATLAB software was applied to find the optimum temperature in which β values of different investigated cases have the least

Table 5. The result of multiobjective optimization with genetic algorithm and standard deviation on β values

Index	T (K)	C_3H_8/PEO	CO_2/PEO	CO_2/PET Low T	CO_2/PET High T	CO_2/i-PP Low T	CO_2/i-PP High T	CO_2/PMMA	CO_2/PEMA	Standard deviation (SD)
1	273.0	0.534	0.496	0.616	0.981	0.475	0.684	0.361	0.743	0.180
2	273.3	0.531	0.495	0.615	0.978	0.474	0.683	0.361	0.743	0.180
3	290.8	0.359	0.413	0.556	0.873	0.442	0.649	0.349	0.720	0.177
4	316.6	0.163	0.304	0.495	0.641	0.396	0.603	0.328	0.688	0.173
5	328.2	0.536	0.260	0.478	0.541	0.375	0.585	0.317	0.673	0.133
6	336.1	0.506	0.231	0.470	0.474	0.362	0.573	0.308	0.663	0.133
7	347.3	0.479	0.192	0.463	0.381	0.342	0.558	0.296	0.650	0.138
8	361.9	0.962	0.145	0.464	0.264	0.318	0.539	0.278	0.632	0.244
9	380.7	---	0.091	0.479	0.284	0.286	0.519	0.252	0.609	0.167
10	445.5	0.176	0.984	0.758	---	0.185	0.476	0.141	0.532	0.299
11	451.4	0.216	0.976	0.755	---	0.176	0.474	0.130	0.525	0.294
12	461.0	0.290	0.969	0.751	---	0.161	0.472	0.110	0.513	0.290
13	515.4	0.879	---	0.730	---	0.084	0.476	---	0.451	0.272
14	527.7	---	---	0.725	---	0.067	0.481	---	0.438	0.235
15	533.0	---	---	0.727	---	0.070	0.465	---	0.459	0.235

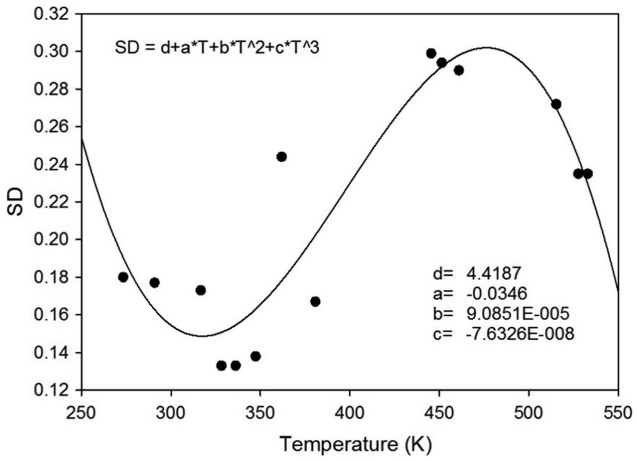

Fig. 11. The cubic polynomial fitting for standard deviations of β versus temperature.

standard deviation. Note that during optimization with settings presented in Table 1, unacceptable β values were also reported by the software which all were excluded in standard deviation calculations. The raw optimization results MAT file generated by MATLAB software can be found in the supplementary material.

From the optimization toolbox of MATLAB, 'gamultiobj' solver was selected; the fitness function was addressed to the toolbox with one variable (T) and in the constraint entry the lower bond (273 K) and upper bond (533 K) for temperatures consideration in optimization were defined. The results of multi-objective optimization are presented in Table 5.

As can be seen, the least standard deviation between β values is related to temperatures of 328.2 and 336.1 K. Thus, in this temperature, the β values are less disperse and closer to each other and these temperatures can be suggested as optimum temperatures at which the proposed model can predict the solubilities of gases in polymers more accurately. The trend of change of standard deviations shows that at lower temperatures, there are smaller deviations between determined k_T values. A data fitting for standard deviation of β values versus temperature is presented in Fig. 11.

As can be seen, there is good agreement (R^2=0.8367) between fitted polynomial with data points from GA. The fitted cubic function of temperature has a minimum at 317 K, and at this temperature the minimum value of standard deviation is 0.148. Based on the correlation obtained, at 317 K the model predicts the solubilities of gases in polymers with its highest accuracy if one unified β value has to be selected for solubility estimations.

To evaluate the solubility prediction power of the proposed modified NELF model and compare it with the performance of the NELF model, the chi-square test was applied to each gas/polymer system considered in this work. The calculation of the solubility coefficient of the NELF model was performed using method proposed by Shoghl et al. [33].

The chi-square test statistic is fundamentally the sum of the squares of the differences between the experimental data and data extracted from models, with each square difference divided by the corresponding data obtained by calculating from models. It is mathematically defined as:

Table 6. The calculated chi-square values of NELF and modified NELF model for different gas/polymer systems

Gas/Polymer system	χ^2	
	NELF model	Modified NELF model
C_3H_8/PEO	0.00820	0.00258
CO_2/PEO	0.03734	0.01571
CO_2/PET (high T)	0.00178	0.00021
CO_2/PET (low T)	0.05195	0.01106
CO_2/i-PP (high T)	0.00573	0.00221
CO_2/i-PP (low T)	0.03531	0.00265
CO_2/PEI	0.05884	0.02263
CO_2/PMMA	0.01241	0.00278
CO_2/PEMA	0.06552	0.01335

$$\chi^2 = \sum_{i=1}^{n} \frac{(S_{ei} - S_{mi})^2}{S_{mi}} \quad (14)$$

where n is the number of solubility coefficient data points, S_{ei} is the i^{th} experimental solubility coefficient at determined pressure and temperature, and S_{mi} is the i^{th} solubility coefficient extracted from the prediction by NELF model and by the proposed modified NELF model at the same determined pressure and temperature which S_{ei} was reported. If there will be a great agreement between experimental data and model predictions, the χ^2 value will be a small number (ideally near zero); however, as the deviation of the model from experimental data increases, the χ^2 value becomes larger. Hence, it is necessary to analyze the data set on the chi-square test to confirm the best-fit model for prediction of gas solubility in different polymers.

The calculated chi-square values of NELF and modified NELF model for investigated gas/polymer pairs are presented in Table 6. Note that the chi-values for each gas/polymer pair in this table were calculated based on the whole experimental and related modeling data points reported at different pressures and temperatures and presented in Figs. 2-10.

As can be seen, although the calculated values of χ^2 for both NELF and modified NELF model are small numbers, the χ^2 values related to the modified NELF model in all of the investigated cases are smaller than those related to NELF model. This demonstrates that the solubility prediction ability of modified NELF model is superior to the NELF, at least for the gas/polymer system involved in this study. Thus, the introduction of a correction factor of fractional free volume in the calculation of solubility of gases in polymers by NELF model leads to enhancement in the prediction power of this model.

CONCLUSION

For improved prediction of C_3H_8 and CO_2 solubilities in different polymers, a novel NELF modified model based on introduction of fractional free volume correction factor (β) and depth of diffusion (ζ) in the calculation of solubility coefficient (S) from infinite dilution solubility coefficient (S_0) was proposed. In all of the investigated gas/polymer systems, the value of β decreased with temperature due to increased sorption capacity of polymers as a

result of the decrease in imposed hypothetical pressure on polymer chain and increase in fractional free volume of polymers. In most of the investigated gas/polymer systems, the value of β also decreased or remained constant with increase in ζ except for the CO_2/PET case which experienced the opposite trend of change due to the initiation of crystallization of amorphous phase of PET, which results if there is formation of a phase with reduced high affinity for CO_2 sorption. The results of multi-objective optimization with genetic algorithm showed that at 328.2 and 336.1 K the fractional free volume correction factor less disperses more close to each other for all gas/polymer pairs investigated. The correlation of standard deviations of fractional free volume correction factors with temperature revealed that 317 K was the optimum temperature at which the highest accuracy of solubility prediction is possible. The comparison of the performance of the NELF model and modified NELF model of this work by the aid of chi-square test showed the supremacy of the proposed NELF model in this work with considerably smaller χ^2 values.

This work successfully modified the NELF model based on two adjustable parameters, β and ζ. The β value can be easily calculated based on experimental and modeling data available in the literature; however, reports regarding the systematic calculation of depth of diffusion of penetrant in polymers are rare, hence this parameter was considered as an independent variable in determination of β. It would be very useful to derive an expression in future works for depth of diffusion based on rheological parameters of polymer, operational conditions and physical and thermodynamic properties of penetrant to try to reduce the number of adjustable parameters in modified NELF model and generalize the application of this model for wide variety of gas/polymer systems.

FUNDING

This research did not receive any specific grant from funding agencies in the public, commercial or not-for-profit sectors.

NOMENCLATURE

English Letters

A : total Helmholtz free energy [J]
a^{NE} : Helmholtz free energy density at nonequilibrium state [J mol^{-1}]
N : numbers of moles of penetrants
R : Universal gas constant [J mol^{-1} K^{-1}]
T^* : characteristic temperature of the mixture of gases [K]
T_i^* : characteristic temperature of pure component i [K]
$\tilde{T}$: dimensionless temperature
r : molar average number of lattice sites occupied by a molecule in the mixture
r_i : molar number of lattice sites occupied in the mixture by molecules of species i
r_i^0 : number of lattice sites occupied by a mole of pure component i
v_i^* : volume occupied by a mole of lattice sites of pure substance [m^3 mol^{-1}]
S_0 : infinite dilution solubility coefficient [m^3(STP) m^{-3} Pa]
p_i^* : characteristic pressure of pure component i [Pa]
$\Delta p_{i,j}^*$: pressure binary interaction parameter between penetrants i and j [Pa]
C_1 : concentration of penetrant in matrix of polymer [mol m^{-3}]
M_i : molecular weight of penetrant (i=1) or polymer (i=2) [kg mol^{-1}]
j_1 : molecular flux of penetrant in polymer [mol m^{-2} s^{-1}]
D_{12} : diffusion coefficient of penetrant in polymer [m^2 s^{-1}]
S : diffusion coefficient of solute in polymer [kg_{solute}.$kg_{polymer}^{-1}$]
r_{12} : molecular separation at collision [nm]
k : Boltzmann constant
f : fractional free volume [FFV]
z : the direction of diffusion [μm]

Greek Letters

$\tilde{\rho}$: dimensionless density [kg m^{-3}]
ρ^* : lattice fluid characteristic density [kg m^{-3}]
ρ_i^* : characteristic density of pure component i [kg m^{-3}]
ρ_2^0 : density of polymer in very low pressures [kg m^{-3}]
ρ_i : density of penetrant molecule (i=1), density of polymer (i=2) [kg m^{-3}]
ϕ_i : volume fraction of component i
μ_i^{NE} : non-equilibrium chemical potential of component i [J mol^{-1}]
Ψ : binary adjustable parameter
ε_{12} : energy of molecular attraction [kg m^{-2} s^{-2}]
β : fractional free volume correction factor
ζ : depth of diffusion of penetrant in polymer matrix [μm]
χ^2 : chi-square value

REFERENCES

1. E. Nezhadmoghadam, M. P. Chenar, M. Omidkhah, A. Nezhadmoghadam and R. Abedini, *Korean J. Chem. Eng.*, **35**, 526 (2018).
2. A. R. Kamble, C. M. Patel and Z. Murthy, *Sep. Sci. Technol.*, **54**, 311 (2019).
3. M. H. Nematollahi, S. Babaei and R. Abedini, *Korean J. Chem. Eng.*, **36**, 763 (2019).
4. E. Jiaqiang, X. Zhao, Y. Deng and H. Zhu, *Appl. Therm. Eng.*, **93**, 166 (2016).
5. C. Wang, X. Sun and J. Zhang, *Appl. Therm. Eng.*, **156**, 562 (2019).
6. E. Shi, X. Zang, C. Jiang and M. Mohammadpourfard, *J. Therm. Anal. Calorim.* (2019), https://doi.org/10.1007/s10973-019-08556-3.
7. E. Shi, F. Jabari, A. Anvari-Moghaddam, M. Mohammadpourfard and B. Mohammadi-Ivatloo, *Appl. Sci.*, **9**, 1925 (2019).
8. E. Jiaqiang, X. Zhao, H. Liu, J. Chen, W. Zuo and Q. Peng, *Appl. Energy*, **175**, 218 (2016).
9. A. Dashti, H. R. Harami and M. Rezakazemi, *Int. J. Hydrogen Energy*, **43**, 6614 (2018).
10. S. Maghami, A. Mehrabani-Zeinabad, M. Sadeghi, J. Sánchez-Laínez, B. Zornoza, C. Téllez and J. Coronas, *Chem. Eng. Sci.*, **205**, 58 (2019).
11. B. Chen, Y. Dai, X. Ruan, Y. Xi and G. He, *Front. Chem. Sci. Eng.*, **12**, 296 (2018).
12. M. A. Khansary, *Korean J. Chem. Eng.*, **33**, 1402 (2016).
13. E. Toni, M. Minelli and G. C. Sarti, *Fluid Phase Equilib.*, **455**, 54 (2018).

14. M. Rezakazemi and S. Shirazian, *Int. J. Hydrogen Energy*, **43**, 22357 (2018).
15. K. von Konigslow, C. B. Park and R. B. Thompson, *Soft Matter*, **14**, 4603 (2018).
16. E. Ricci, A. E. Gemeda, N. Du, N. Li, M. G. De Angelis, M. D. Guiver and G. C. Sarti, *J. Membr. Sci.*, **585**, 136 (2019).
17. L. Liu and S. E. Kentish, *J. Membr. Sci.*, **553**, 63 (2018).
18. Y. Lou, P. Hao and G. Lipscomb, *J. Membr. Sci.*, **455**, 247 (2014).
19. F. Doghieri and G. C. Sarti, *Macromolecules*, **29**, 7885 (1996).
20. M. De Angelis, G. Sarti and F. Doghieri, *J. Membr. Sci.*, **289**, 106 (2007).
21. M. Minelli and M. G. De Angelis, *Fluid Phase Equilib.*, **367**, 173 (2014).
22. M. Minelli, *J. Membr. Sci.*, **451**, 305 (2014).
23. M. Galizia, Z. P. Smith, G. C. Sarti, B. D. Freeman and D. R. Paul, *J. Membr. Sci.*, **475**, 110 (2015).
24. M. Minelli and F. Doghieri, *Fluid Phase Equilib.*, **381**, 1 (2014).
25. A. Jomekian, R. M. Behbahani, T. Mohammadi and A. Kargari, *Korean J. Chem. Eng.*, **34**, 440 (2017).
26. H. Sanaeepur, S. Mashhadikhan, G. Mardassi, A. E. Amooghin, B. Van der Bruggen and A. Moghadassi, *Korean J. Chem. Eng.*, **36**, 1339 (2019).
27. S.-A. Hoseinpour, A. Barati-Harooni, P. Nadali, A. Mohebbi, A. Najafi-Marghmaleki, A. Tatar and A. Bahadori, *J. Chemom.*, **32**, e2956 (2018).
28. N. A. Menad, A. Hemmati-Sarapardeh, A. Varamesh and S. Shamshirband, *J. CO2 Util*, **33**, 83 (2019).
29. A. Jomekian and S. J. Poormohammadian, *Fluid Phase Equilib.*, **500**, 112261 (2019).
30. M. Minelli, S. Campagnoli, M. De Angelis, F. Doghieri and G. Sarti, *Macromolecules*, **44**, 4852 (2011).
31. M. Minelli, M. G. De Angelis, M. Giacinti Baschetti, F. Doghieri, G. C. Sarti, C. P. Ribeiro Jr. and B. D. Freeman, *Ind. Eng. Chem. Res.*, **54**, 1142 (2015).
32. F. Doghieri and G. C. Sarti, *J. Membr. Sci.*, **147**, 73 (1998).
33. S. N. Shoghl, A. Raisi and A. Aroujalian, *RSC Adv.*, **6**, 57683 (2016).
34. S. N. Shoghl, A. Raisi and A. Aroujalian, *RSC Adv.*, **5**, 38223 (2015).
35. M. Minelli and F. Doghieri, *Ind. Eng. Chem. Res.*, **51**, 16505 (2012).
36. V. Wiesmet, E. Weidner, S. Behme, G. Sadowski and W. Arlt, *J. Supercrit. Fluids*, **17**, 1 (2000).
37. S. Zid, M. Zinet and E. Espuche, *J. Polym. Sci., Part B: Polym. Phys.*, **56**, 621 (2018).
38. A. Thran, G. Kroll and F. Faupel, *J. Polym. Sci., Part B: Polym. Phys.*, **37**, 3344 (1999).
39. W. Koros and D. R. Paul, *J. Polym. Sci., Part B: Polym. Phys.*, **16**, 1947 (1978).
40. W. Koros and D. R. Paul, *J. Polym. Sci., Part B: Polym. Phys.*, **16**, 2171 (1978).
41. W. Koros and D. R. Paul, *Polym. Eng. Sci.*, **20**, 14 (1980).
42. W. Koros, D. R. Paul, M. Fujii, H. Hopfenberg and V. Stannett, *J. Appl. Polym. Sci.*, **21**, 2899 (1977).
43. T. Xia, Z. Xi, T. Liu and L. Zhao, *Chem. Eng. Sci.*, **168**, 124 (2017).
44. D.-c. Li, T. Liu, L. Zhao and W.-k. Yuan, *Ind. Eng. Chem. Res.*, **48**, 7117 (2009).
45. Z. Lei, H. Ohyabu, Y. Sato, H. Inomata and R. L. Smith Jr., *J. Supercrit. Fluids*, **40**, 452 (2007).
46. G. Li, F. Gunkel, J. Wang, C. Park and V. Altstädt, *J. Appl. Polym. Sci.*, **103**, 2945 (2007).
47. J. Chen, T. Liu, L. Zhao and W.-k. Yuan, *Thermochim. Acta*, **530**, 79 (2012).
48. M. M. López-González, V. Compan, E. Saiz, E. Riande and J. Guzman, *J. Membr. Sci.*, **253**, 175 (2005).
49. K. Simons, K. Nijmeijer, J. G. Sala, H. van der Werf, N. E. Benes, T. J. Dingemans and M. Wessling, *Polymer*, **51**, 3907 (2010).
50. M. Wessling, M. L. Lopez and H. Strathmann, *Sep. Purif. Technol.*, **24**, 223 (2001).
51. W. J. Koros, G. N. Smith and V. Stannett, *J. Appl. Polym. Sci.*, **26**, 159 (1981).
52. Z. Lu, Y. Pan, X. Liu, G. Zheng, D. W. Schubert and C. Liu, *Mater. Lett.*, **221**, 62 (2018).
53. Y. Pan, X. Liu, J. Kaschta, X. Hao, C. Liu and D. W. Schubert, *Polymer*, **113**, 34 (2017).